

Computer Vision-Based Method for Quantifying Iron-Related Defects in Silicon Solar Cells

Oleg Olikh, Oleksii Zavhorodnii, Yulia Perets

*Taras Shevchenko National University of Kyiv, 64/13, Volodymyrska Street,
Kyiv, 01601, Ukraine*

olegolikh@knu.ua

SUPPLEMENTARY MATERIAL

I. Initial hyperparameter search space

Abbreviations to denote visual models and their feature extraction outputs:

ENB7:CL - EfficientNetB7, classifier layer output (1000-D).

ENB7:FE - EfficientNetB7, feature extractor output (2560-D).

ENB7:FE:P - EfficientNetB7, feature extractor output with PCA reduction (39-D).

MNV2:CL - MobileNetV2, classifier layer output (1000-D).

MNV2:FE - MobileNetV2, feature extractor output (1280-D).

MNV2:FE:P - MobileNetV2, feature extractor output with PCA reduction (124-D).

NAS:CL - NASNetLarge, classifier layer output (1000-D).

NAS:CL:P - NASNetLarge, classifier layer output with PCA reduction (30-D).

NAS:FE - NASNetLarge, feature extractor output (4032-D).

R152:CL - ResNet152V2, classifier layer output (1000-D).

R152:FE - ResNet152V2, feature extractor output (2048-D).

XCP:CL - Xception, classifier layer output (1000-D).

XCP:FE - Xception, feature extractor output (2048-D).

YL:FE1 - YOLOv4 (CSPDarknet53 backbone), raw feature extractor (top layer, 86528-D).

YL:FE1:P - YOLOv4 (CSPDarknet53 backbone), raw feature extractor with PCA (137-D).

YL:FE2 - CSPDarknet53 backbone, raw feature extractor (top & penultimate layers, 433640-D).

YL:FE2:P - CSPDarknet53 backbone, raw feature extractor with PCA (142-D).

YL:FP1 - YOLOv4, global average pooled features from the top layer (512-D).

YL:FP2 - YOLOv4, concatenated pooled features from the top & penultimate layers (1024-D)

Table S1. Search space of hyperparameters for RF

Hyperparameter	Values
# estimators	[100; 1200]
max depth	[10; 95]
min samples leaf	[1; 15]
min samples split	[2; 16]
bootstrap	True, False
max features	'log2', 'sqrt', [0.05; 1.0]

Table S2. Search space of hyperparameters for GB

Hyperparameter	Values
# estimators	[100; 1200]
max depth	[15; 90]
min samples leaf	[1; 15]
min samples split	[2, 16]
learning rate	[10^{-3} , 10^{-1}]
max features	'log2', 'sqrt', [0.05; 1.0]

Table S3. Search space of hyperparameters for SVR

Hyperparameter	Values
kernel	linear, poly, rbf, sigmoid
Degree*	[2; 6]
C0	[0; 15]
Tolerance	[10^{-6} ; 10^{-2}]
C	[10^{-2} ; 15]
Epsilon	[10^{-3} ; 1]

* for poly kernel only

Table S4. Search space of hyperparameters for XGB

Hyperparameter	Values
booster	gbtree, gblinear, dart
max depth*	[2, 10]
min split loss*	[0; 5]
min child weight*	[0; 5]
subsample*	[0.1; 1.0]
colsample by tree*	[0.1; 1.0]
# estimators	[200; 1700]
learning rate	[10^{-5} ; 1]
L1	[10^{-9} ; 1]
L2	[10^{-8} ; 1]

* for all boosters except gblinear

Table S5. Search space of hyperparameters for DNN

Hyperparameter	Values
hidden layers configuration	[512, 256, 128, 64]
activation function*	ReLU, sigmoid, tanh, SELU, ELU
Optimizer*	SGD, RMSprop, Adam, Adadelta, Adagrad, Adamax, Nadam, Ftrl
learning rate	[10^{-5} ; 10^{-2}]
weight initializer*	Xavier Normal (XN), Xavier Uniform (XU), He Normal (HN), He Uniform (HU), Random Normal (RN), Random Uniform (RU)
Regularizer	None, L1, L2
RegRate**	[10^{-5} ; 10^{-1}]
DropoutNeeded	True, False
DropRate***	[0.1; 0.5]
LayerNormalization	True, False

* all activation functions, optimizers, and weight initializations used in this work correspond to standard implementations available in the Keras deep learning framework

** for Regularizer \neq None

*** for DropoutNeeded = True

II. Selected hyperparameter combinations

Table S6. Chosen rational hyperparameter combinations for RF models

Visual Model	Hyperparameter					
	# estimators	max depth	min sample split	min sample leaf	max features	bootstrap
ENB7:CL	750	35	3	2	0.2	False
ENB7:FE	900	40	4	2	0.2	False
ENB7:FE:P	460	54	4	1	1	True
MNV2:CL	450	20	4	1	0.1	False
MNV2:FE	460	50	3	1	0.05	False
MNV2:FE:P	500	85	5	3	0.5	False
NAS:CL	395	59	2	1	0.2	False
NAS:CL:P	1175	70	2	1	0.4	False
NAS:FE	750	10	2	1	0.1	False
R152:CL	640	40	4	2	0.4	False
R152:FE	367	38	2	1	sqrt	False
XCP:CL	640	90	2	1	0.2	False
XCP:FE	820	48	4	1	0.1	False
YL:FP1	960	75	4	1	0.4	False
YL:FP2	650	70	2	1	0.2	False
YL:FE2:P	475	45	3	1	0.5	False
YL:FE1:P	425	45	10	1	0.5	False

Table S7. Chosen rational hyperparameter combinations for GB models

Visual Model	Hyperparameter					
	# estimators	max depth	min sample split	min sample leaf	max features	LR
ENB7:CL	750	20	7	11	0.1	3.4e-02
ENB7:FE	750	50	6	9	0.3	4.2e-02
ENB7:FE:P	680	25	4	15	1	3.9e-02
MNV2:CL	1100	40	10	3	sqrt	1.0e-02
MNV2:FE	890	50	12	2	sqrt	1.4e-02
MNV2:FE:P	575	60	4	12	0.6	2.8e-02
NAS:CL	850	70	13	15	0.3	4.8e-02
NAS:CL:P	675	80	11	13	0.4	3.8e-02
NAS:FE	650	67	5	3	0.1	1.3e-02
R152:CL	700	55	8	1	0.4	1.1e-01
R152:FE	640	85	3	7	sqrt	2.3e-02
XCP:CL	470	25	2	6	sqrt	5.2e-02
XCP:FE	760	75	10	4	0.1	2.9e-02
YL:FP1	1160	75	2	8	0.1	3.9e-02
YL:FP2	900	54	3	6	0.2	2.3e-02
YL:FE2:P	750	55	4	7	0.4	1.9e-02
YL:FE1:P	850	55	2	10	0.7	1.2e-02

Table S8. Chosen rational hyperparameter combinations for XGB models

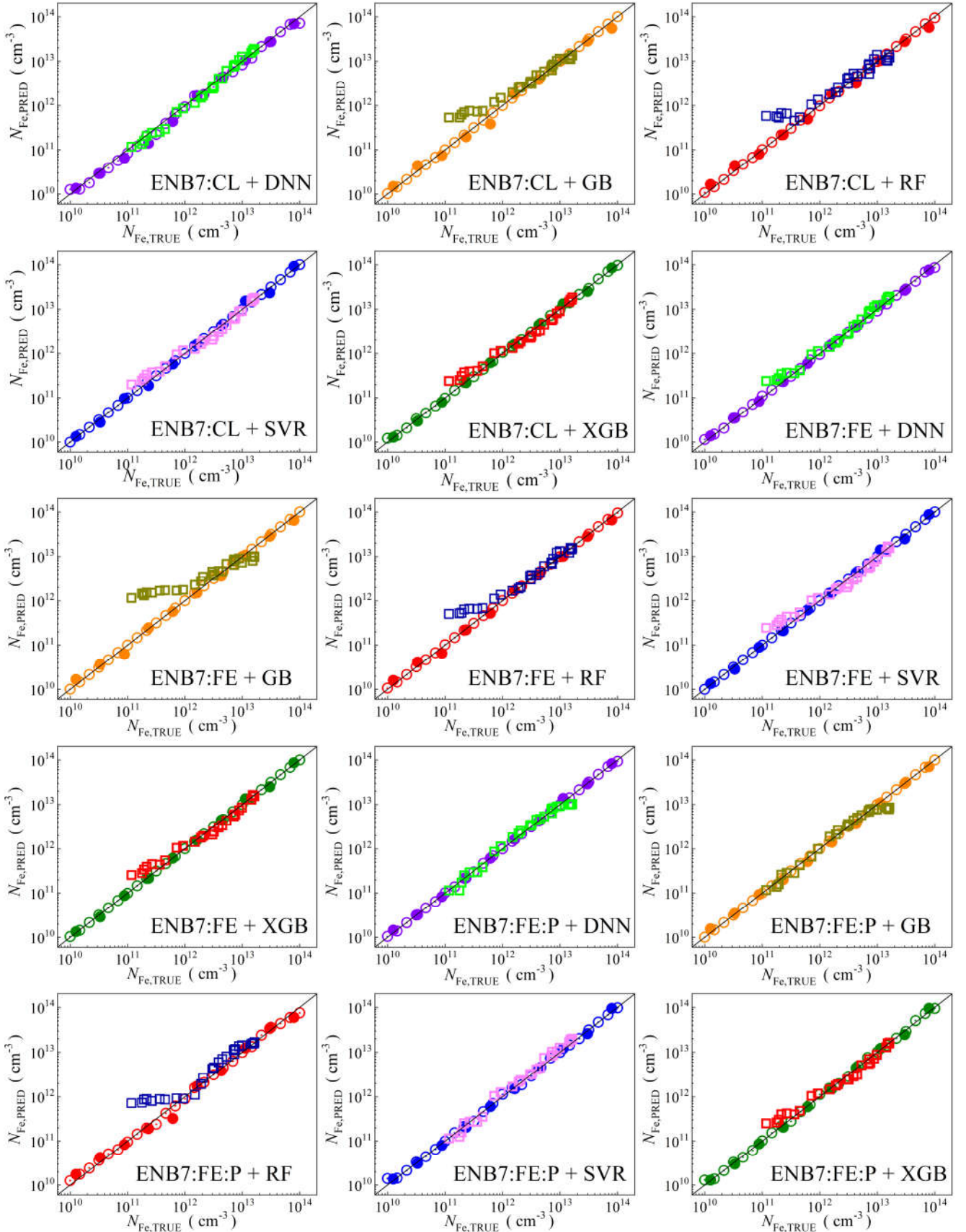
Visual Model	Hyperparameter									
	booster	max depth	min split loss	min child weight	sub sample	colsample bytree	# estimators	LR	L1	L2
ENB7:CL	gblinear	3	--	--	--	--	1080	1.1e-1	1.8e-7	8.4e-4
ENB7:FE	gblinear	3	--	--	--	--	1150	3.2e-1	3.8e-8	2.6e-3
ENB7:FE:P	gblinear	3	--	--	--	--	1640	1.6e-1	5.9e-9	1.4e-2
MNV2:CL	gblinear	3	--	--	--	--	1040	7.0e-2	5.7e-7	3.1e-3
MNV2:FE	gblinear	3	--	--	--	--	600	1.4e-1	6.1e-8	1.9e-2
MNV2:FE:P	gblinear	3	--	--	--	--	1150	7.4e-2	1.0e-8	1.0e-1
NAS:CL	gblinear	3	--	--	--	--	1050	2.6e-1	9.9e-9	2.3e-3
NAS:CL:P	gblinear	3	--	--	--	--	800	3.8e-2	5.0e-9	1.4e-2
NAS:FE	gblinear	3	--	--	--	--	700	6.9e-2	8.5e-9	6.1e-2
R152:CL	gbtree	8	7.9e-3	5.7e-1	0.4	0.9	825	2.2e-2	1.9e-8	3.3e-3
R152:FE	gblinear	6	--	--	--	--	500	4.4e-1	1.1e-8	1.5e-2
XCP:CL	gblinear	3	--	--	--	--	550	2.0e-1	1.4e-6	1.7e-4
XCP:FE	gblinear	3	--	--	--	--	390	2.2e-1	3.7e-6	9.9e-2
YL:FP1	gblinear	3	--	--	--	--	520	9.4e-2	4.7e-5	2.0e-2
YL:FP2	gblinear	3	--	--	--	--	650	1.7e-1	8.1e-9	1.9e-2
YL:FE2:P	gbtree	5	6.4e-2	3.6	0.9	0.5	1275	8.1e-3	1.9e-8	4.9e-3
YL:FE1:P	gbtree	2	3.2e-1	2.5	0.8	0.9	525	3.5e-2	2.1e-8	6.7e-3

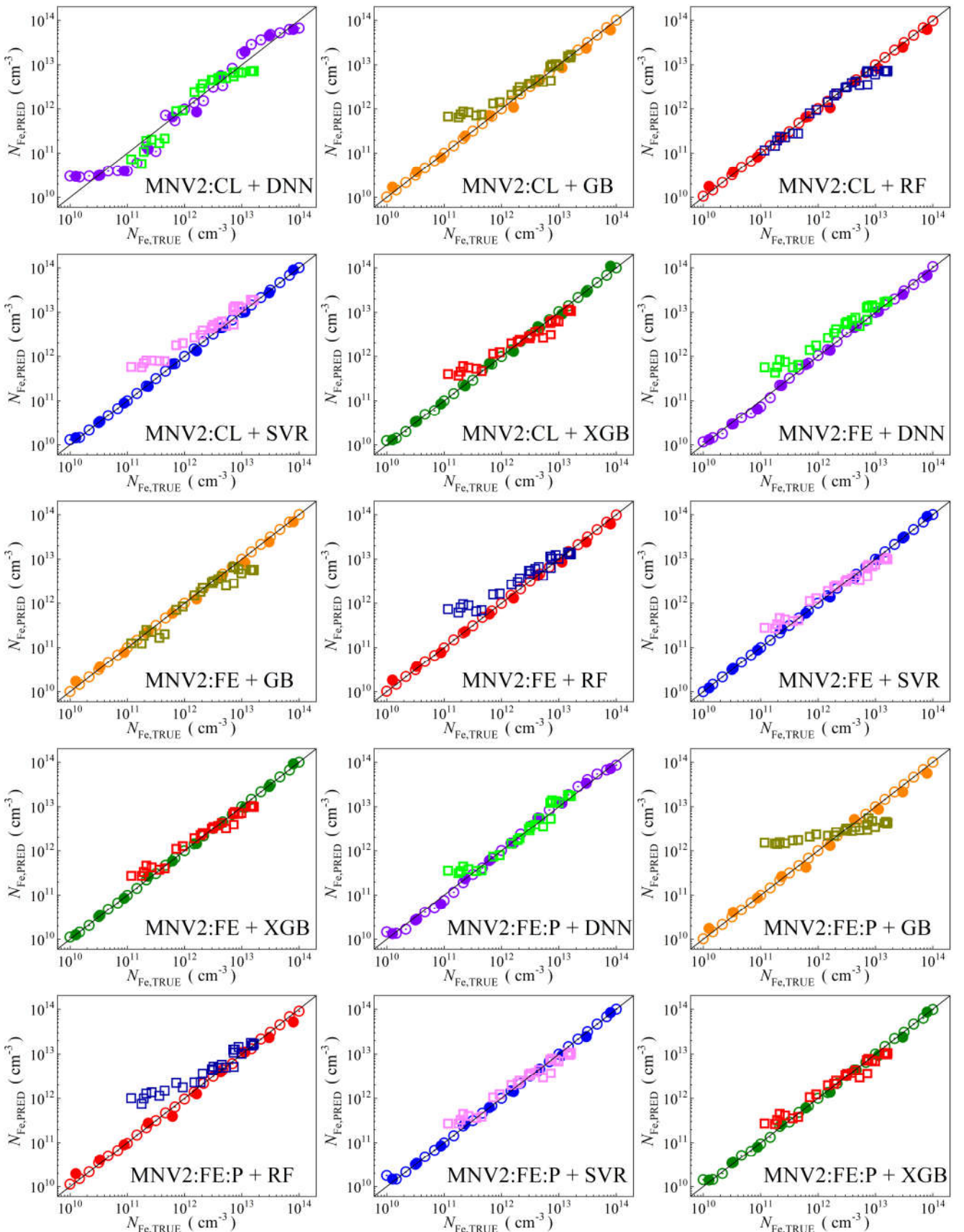
Table S9. Chosen rational hyperparameter combinations for SVR models

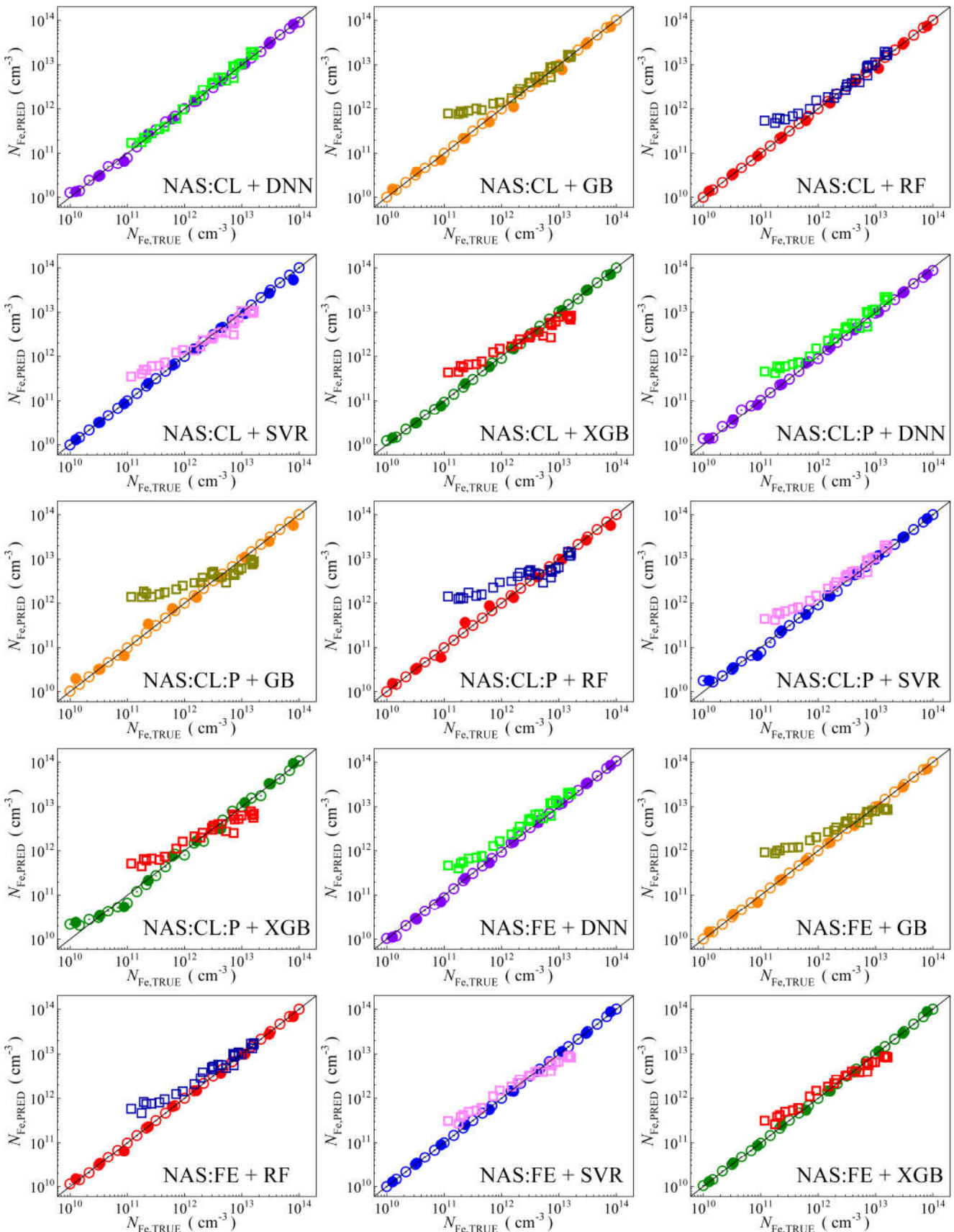
Visual Model	Hyperparameter				
	kernel	C0	Tolerance	C	Epsilon
ENB7:CL	linear	7.79	6.9e-06	2.5	2.2e-05
ENB7:FE	linear	8.29	3.0e-05	2.6	3.5e-05
ENB7:FE:P	linear	10.57	8.4e-04	13.7	2.9e-04
MNV2:CL	rbf	6.80	3.9e-04	10.9	9.6e-05
MNV2:FE	linear	6.54	4.9e-04	6.7	7.1e-05
MNV2:FE:P	linear	7.31	5.2e-04	4.6e-03	8.7e-04
NAS:CL	linear	6.60	4.9e-04	4.6	1.5e-04
NAS:CL:P	rbf	7.17	5.5e-03	11.7	1.5e-04
NAS:FE	linear	5.31	6.5e-04	5.9	2.6e-05
R152:CL	linear	6.66	4.2e-03	2.3	5.4e-05
R152:FE	linear	6.65	1.3e-04	5.2	1.4e-04
XCP:CL	rbf	8.27	7.2e-03	13.8	3.5e-04
XCP:FE	linear	11.24	2.5e-03	9.1	3.8e-04
YL:FP1	rbf	12.61	2.4e-03	6.9	5.6e-05
YL:FP2	rbf	8.30	1.9e-04	9.2	1.4e-05
YL:FE1	linear	8.62	5.3e-04	7.9	1.6e-05
YL:FE2	rbf	11.5	2.3e-05	4.6	6.3e-06
YL:FE2:P	linear	9.18	3.9e-03	2.2	2.4e-04
YL:FE1:P	rbf	7.04	2.7e-03	2.6	2.5e-04

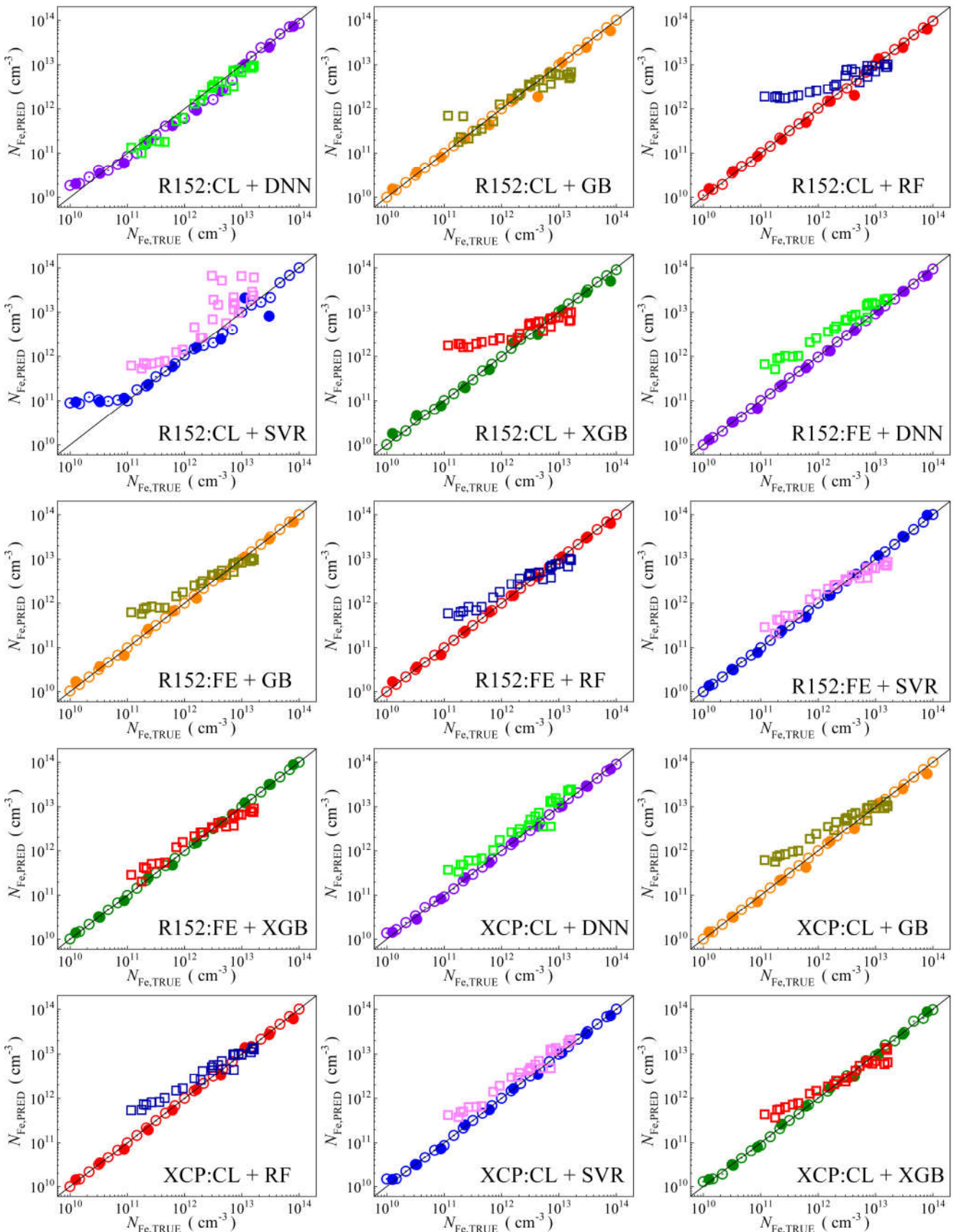
Table S10. Chosen rational hyperparameter combinations for DNN models

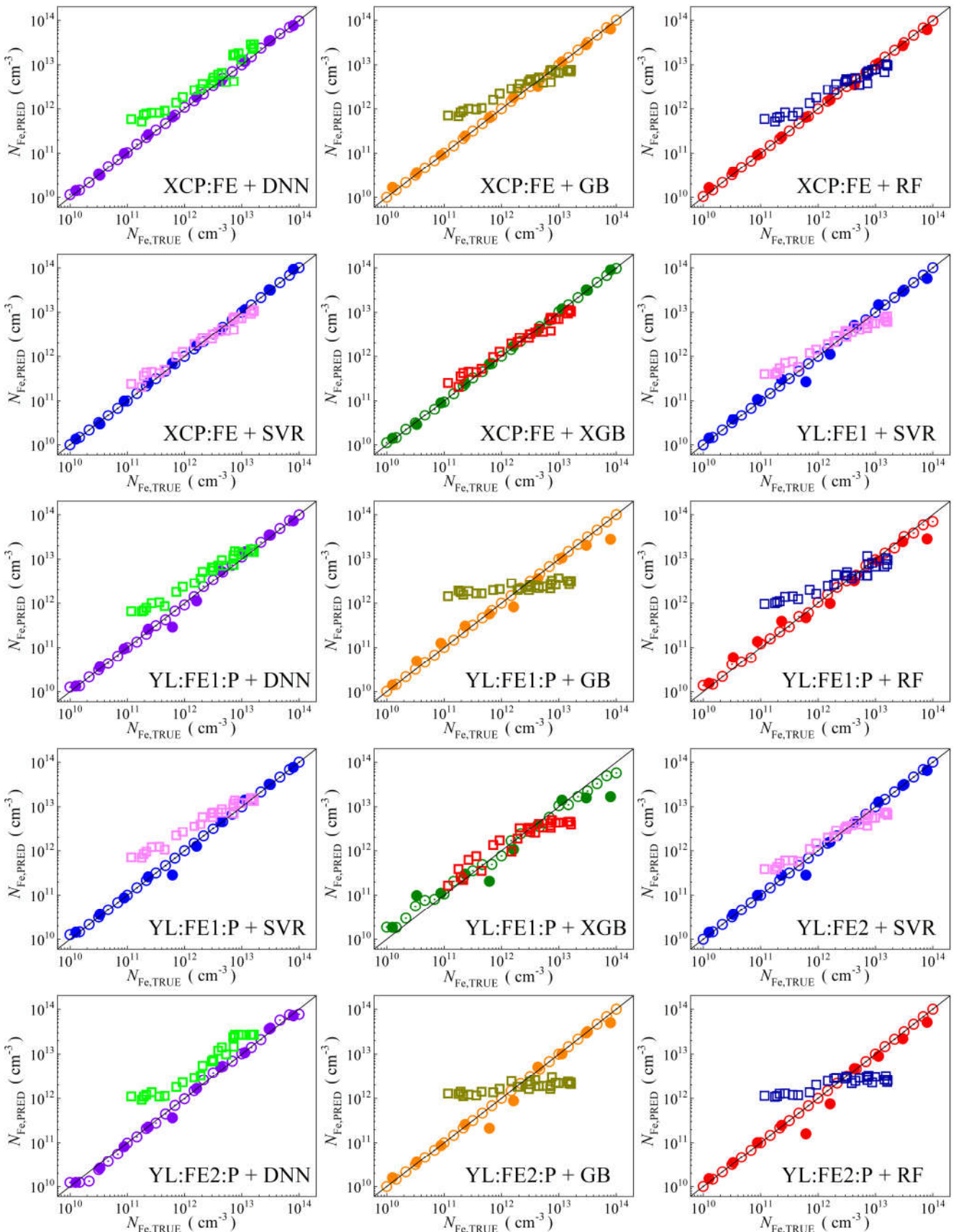
Visual Model	Hyperparameter								
	LR	optimizer	activ. func.	w. init.	Regul.	RegRate	Drop. Need.	Drop. Rate	Layer Norm.
ENB7:CL	3.0e-03	Adam	ELU	HN	None	--	False	--	True
ENB7:FE	1.4e-03	Adamax	SELU	RN	L2	1.0e-03	False	--	True
ENB7:FE:P	1.4e-04	Nadam	SELU	RU	L2	1.0e-03	False	--	True
MNV2:CL	2.4e-03	Nadam	SELU	RN	L2	1.7e-03	True	0.5	True
MNV2:FE	2.8e-03	Nadam	ELU	RN	None	--	False	--	False
MNV2:FE:P	1.3e-04	Adam	tanh	RU	L2	6.4e-04	True	0.4	False
NAS:CL	1.4e-04	Adamax	sigmoid	XU	None	--	False	--	False
NAS:CL:P	3.9e-04	Nadam	tanh	RU	None	--	False	--	True
NAS:FE	4.4e-04	Nadam	SELU	RU	None	--	False	--	True
R152:CL	3.3e-04	Adamax	ELU	RN	L2	2.2e-03	False	--	True
R152:FE	1.1e-03	Nadam	ReLU	HN	None	--	False	--	True
XCP:CL	1.5e-04	Adamax	ReLU	HU	L1	9.7e-04	False	--	True
XCP:FE	2.1e-04	Nadam	sigmoid	XN	L2	8.5e-04	False	--	True
YL:FP1	5.2e-05	Adam	tanh	RU	None	--	False	--	True
YL:FP2	6.9e-04	Adam	SELU	RU	None	--	False	--	True
YL:FE2:P	4.1e-04	Adam	sigmoid	XN	L1	1.3e-04	True	0.2	True
YL:FE1:P	4.3e-04	RMSprop	ELU	XU	L1	5.4e-05	False	--	True











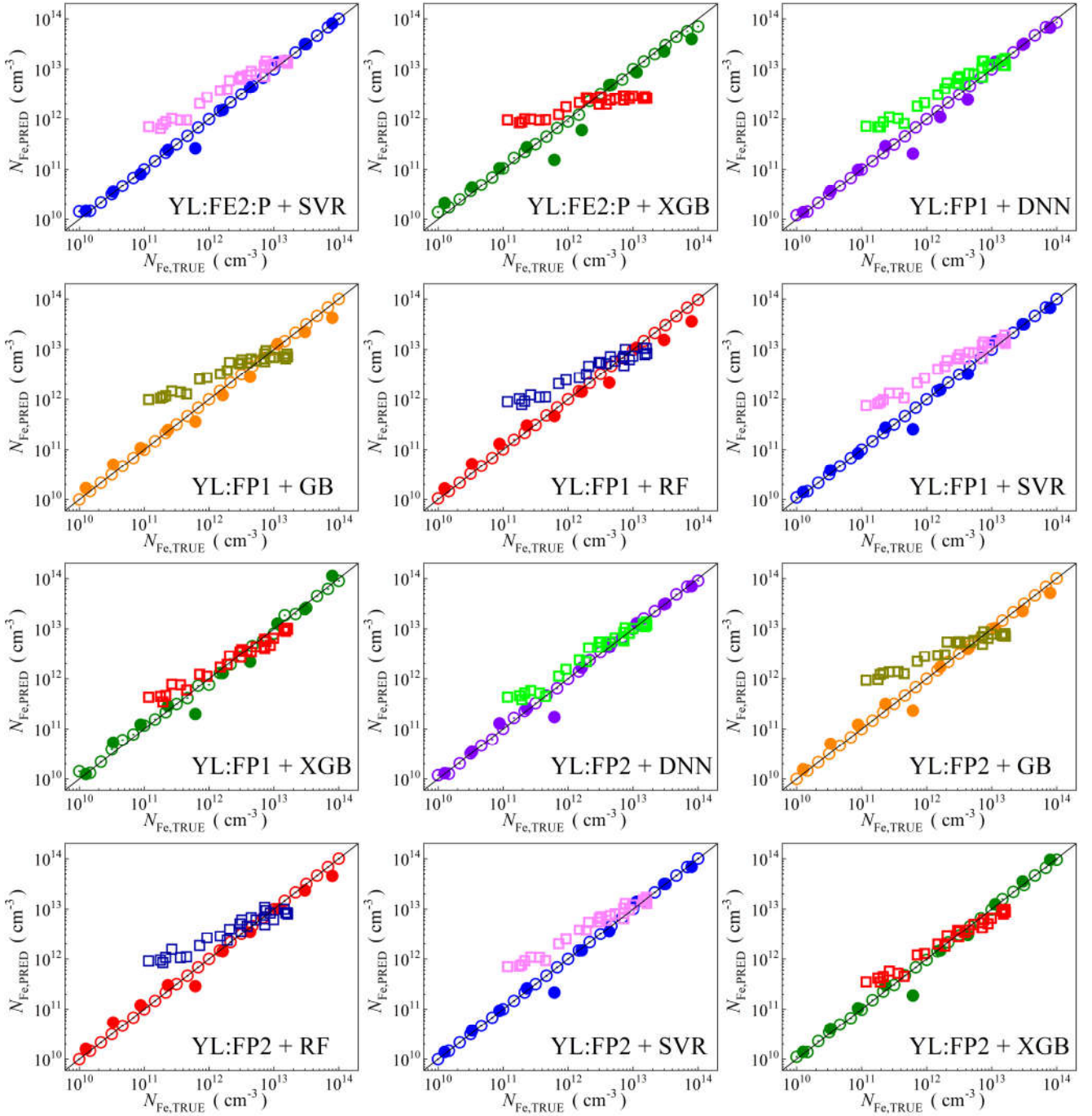


Fig. S1. Scatter plots compare the reference iron $N_{\text{Fe,TRUE}}$ with ML-predicted values $N_{\text{Fe,PRED}}$ obtained using feature vectors extracted from various computer vision models combined with different regression algorithms. The ML models were trained on a simulated dataset. The open circles correspond to the training phase, while the filled circles and open squares correspond to the test phase, representing the simulated and experimental datasets, respectively. The black lines are the identified lines serving as the references.

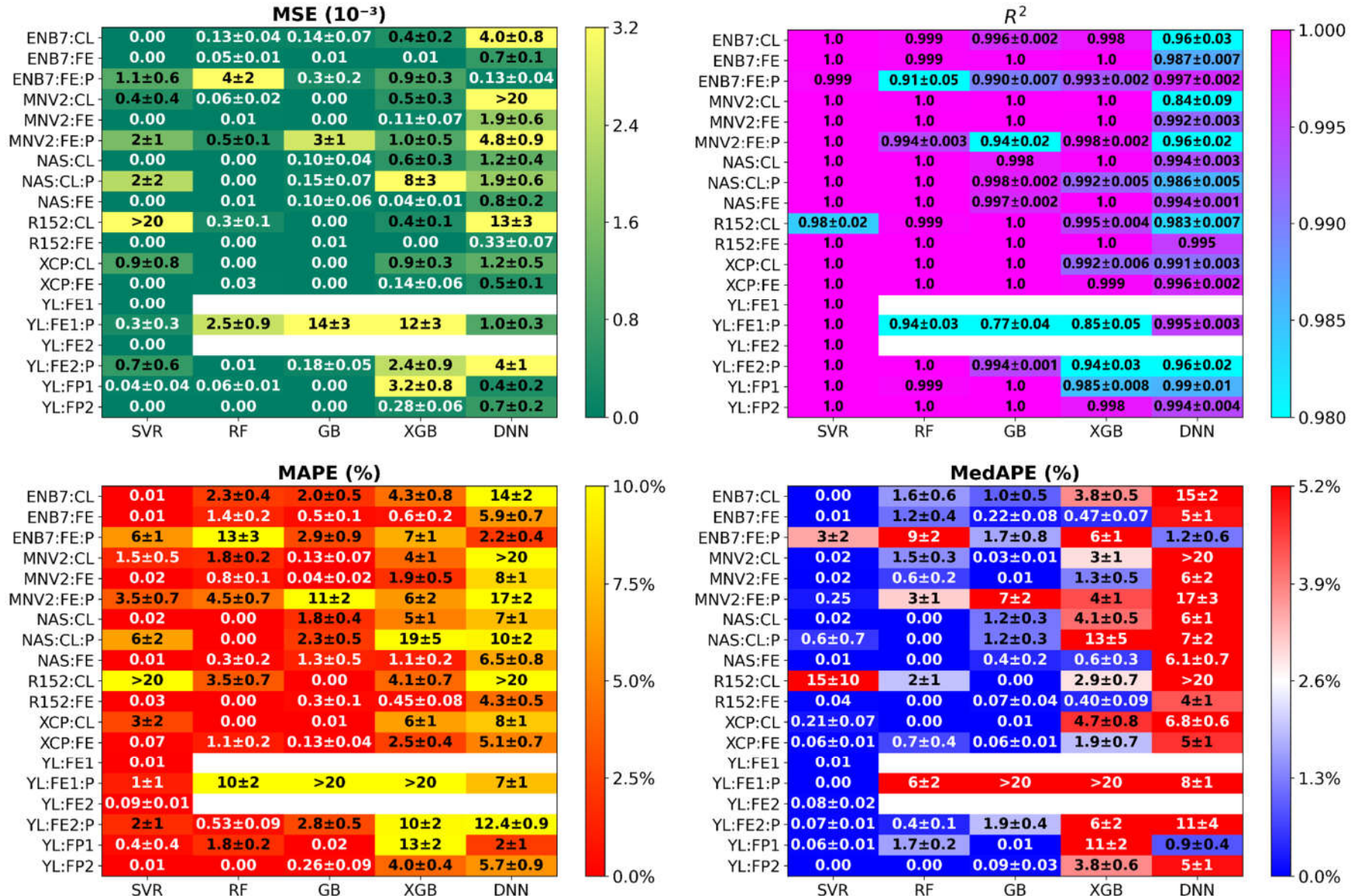


Fig. S2. Mean squared error, coefficient of determination, mean absolute percentage error, and median absolute percentage error for different combinations of computer vision models (vertical axis) and regression models (horizontal axis) during the **training** phase. The models were trained on a **simulated dataset**.

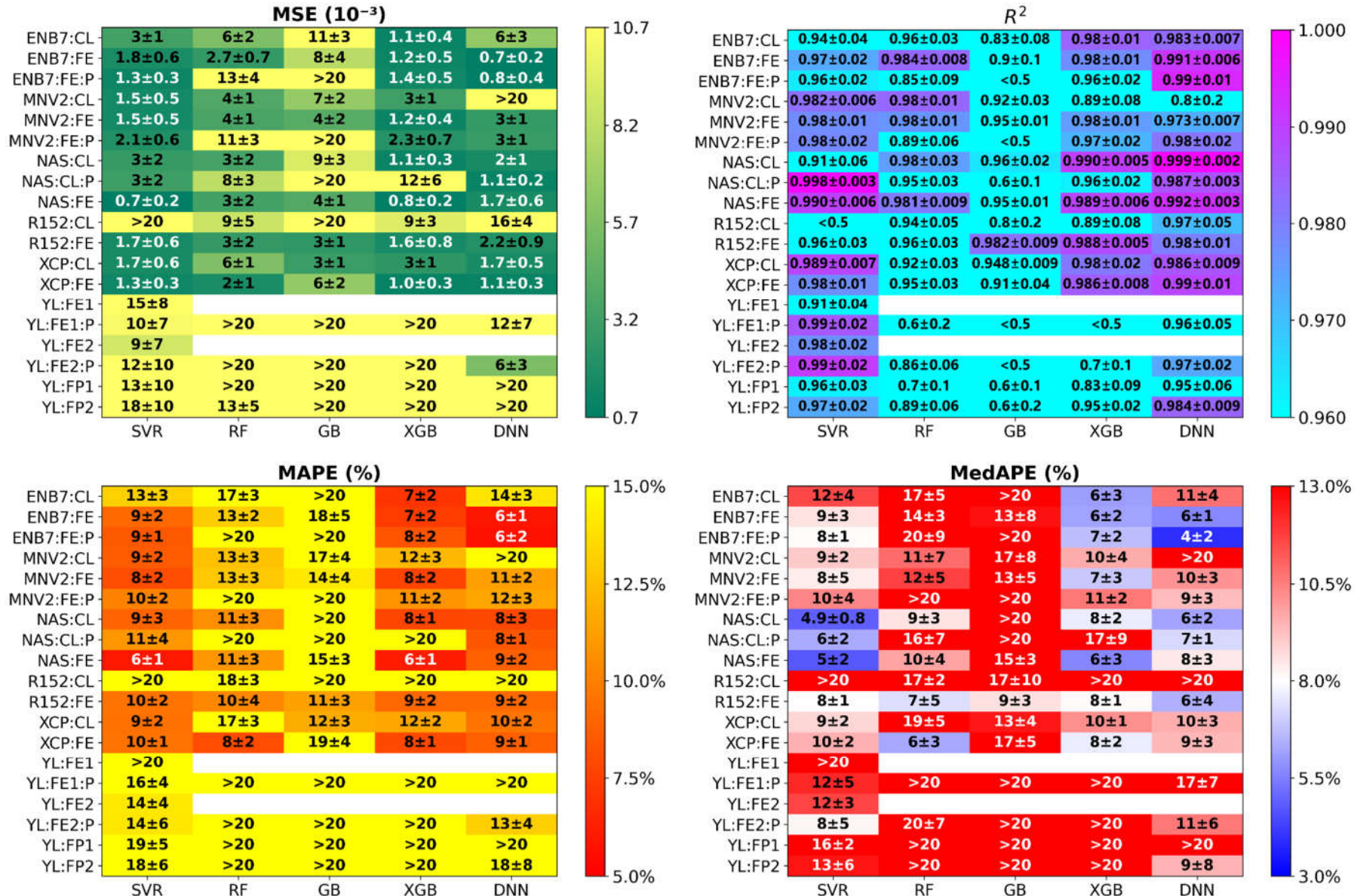


Fig. S3. Mean squared error, coefficient of determination, mean absolute percentage error, and median absolute percentage error for different combinations of computer vision models (vertical axis) and regression models (horizontal axis) during the **test phase with simulated dataset**. The models were trained on a **simulated dataset**.

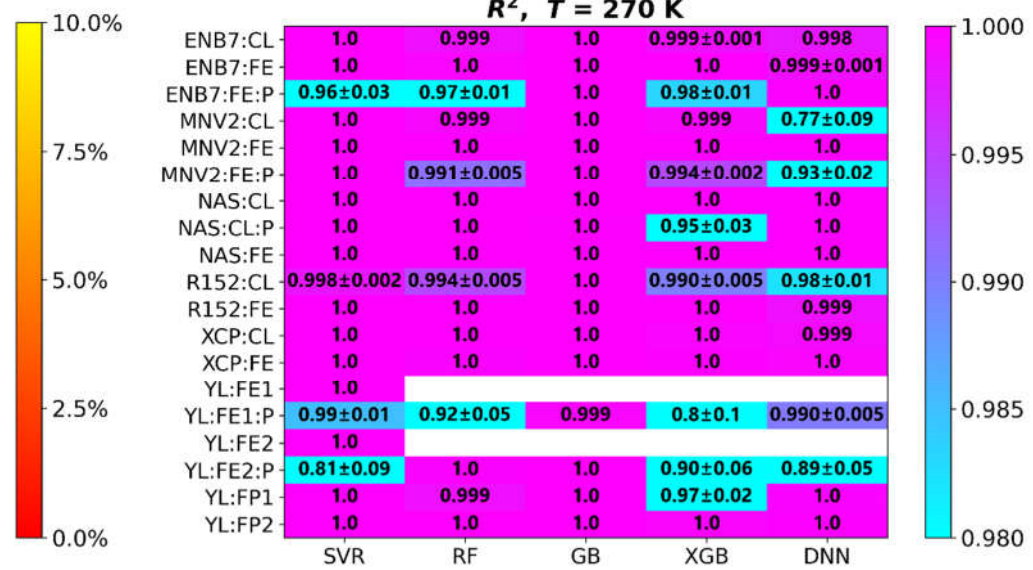
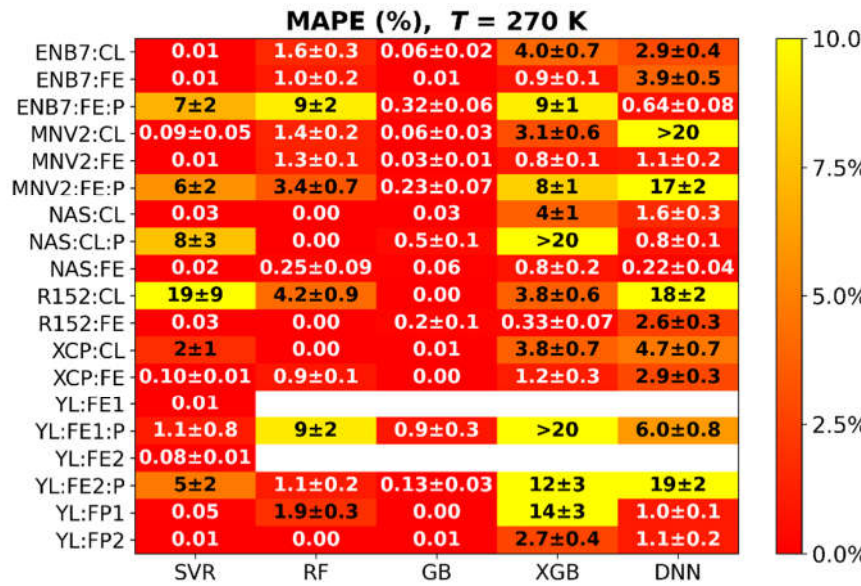
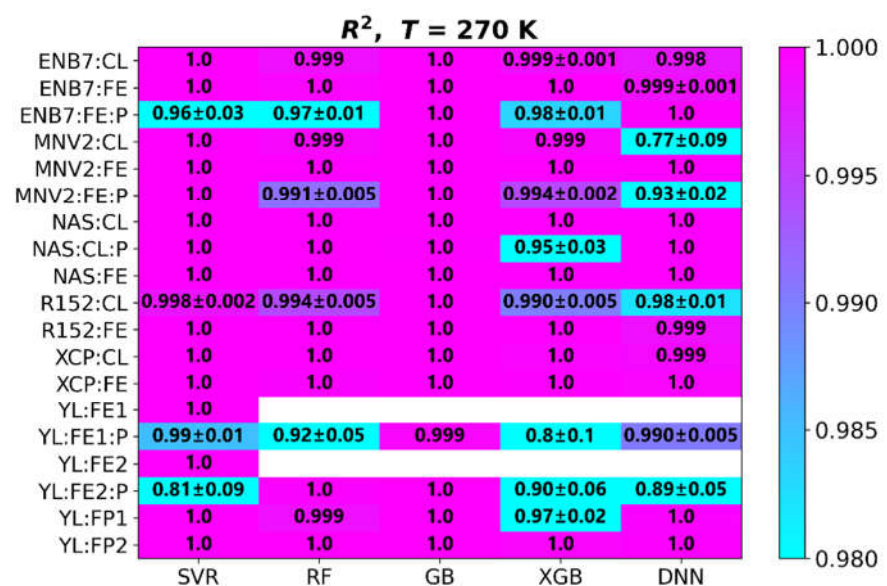
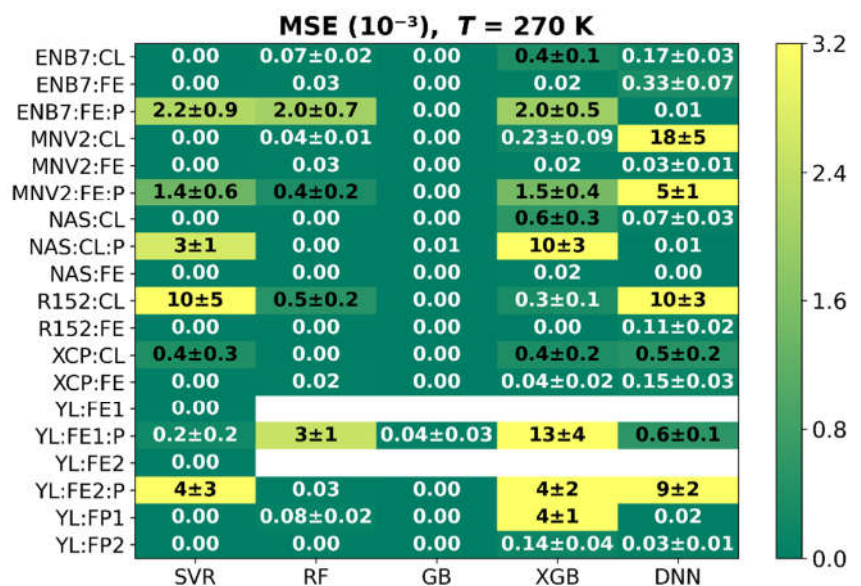


Fig. S4. Mean squared error, coefficient of determination, mean absolute percentage error, and median absolute percentage error for different combinations of computer vision models (vertical axis) and regression models (horizontal axis) during the **training** phase. The models were trained on a **simulated dataset**. Simulations were performed for **270 K**.

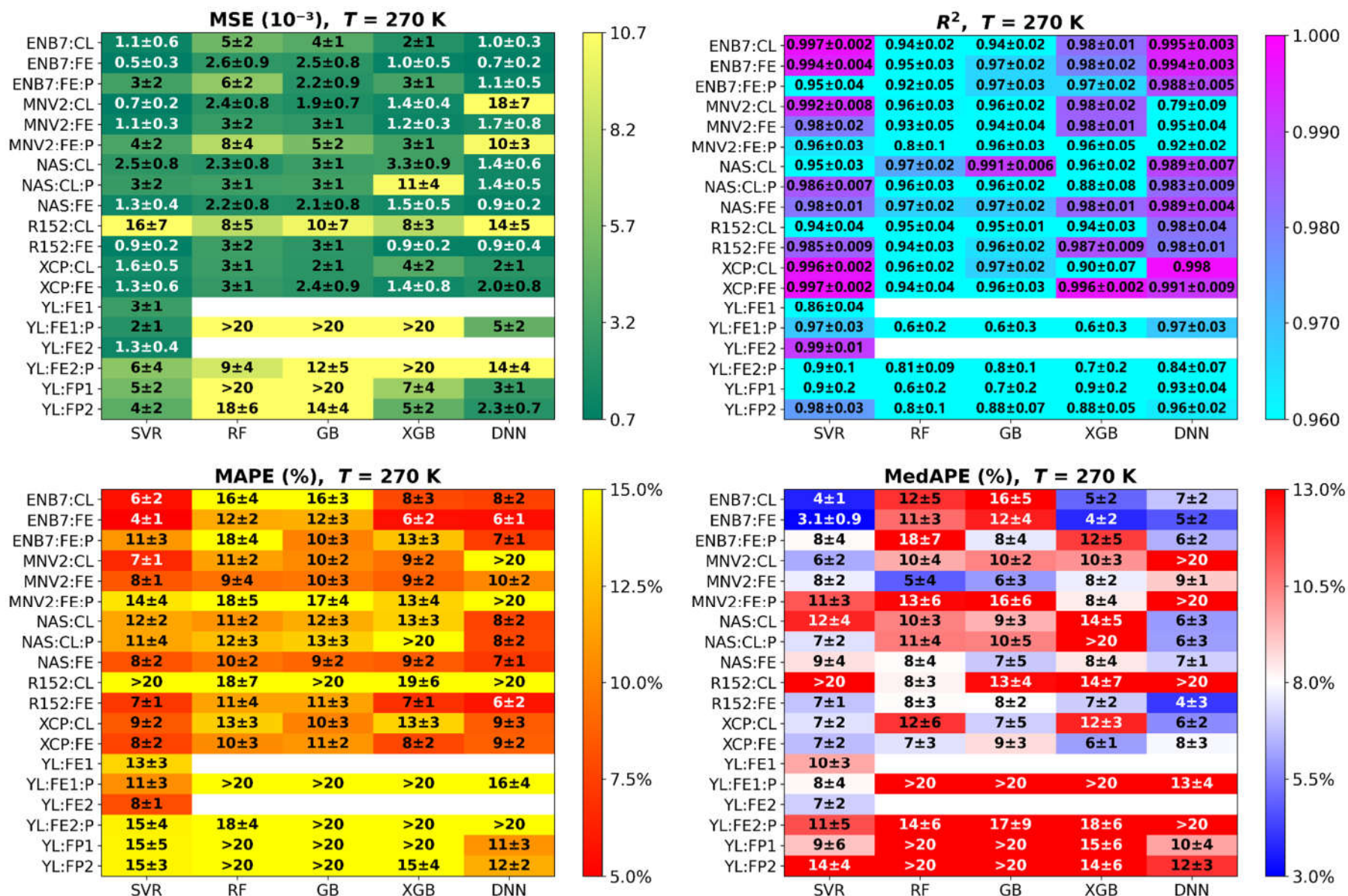


Fig. S5. Mean squared error, coefficient of determination, mean absolute percentage error, and median absolute percentage error for different combinations of computer vision models (vertical axis) and regression models (horizontal axis) during the **test phase with simulated dataset**. The models were trained on a **simulated dataset**. Simulations were performed for **270 K**.

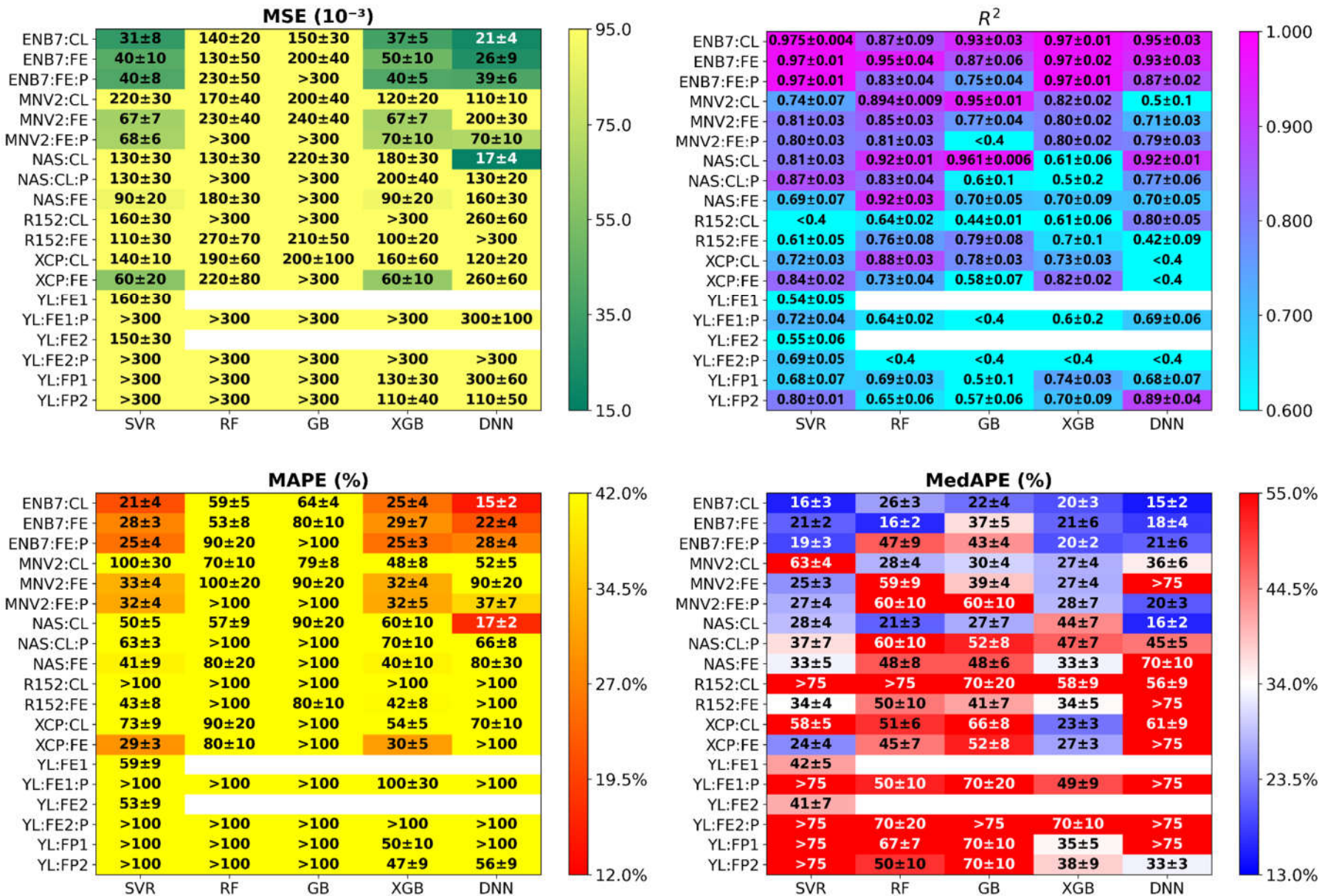


Fig. S6. Mean squared error, coefficient of determination, mean absolute percentage error, and median absolute percentage error for different combinations of computer vision models (vertical axis) and regression models (horizontal axis) during the **test phase with experimental dataset without post-hoc calibration**. The models were trained on a **simulated dataset**.

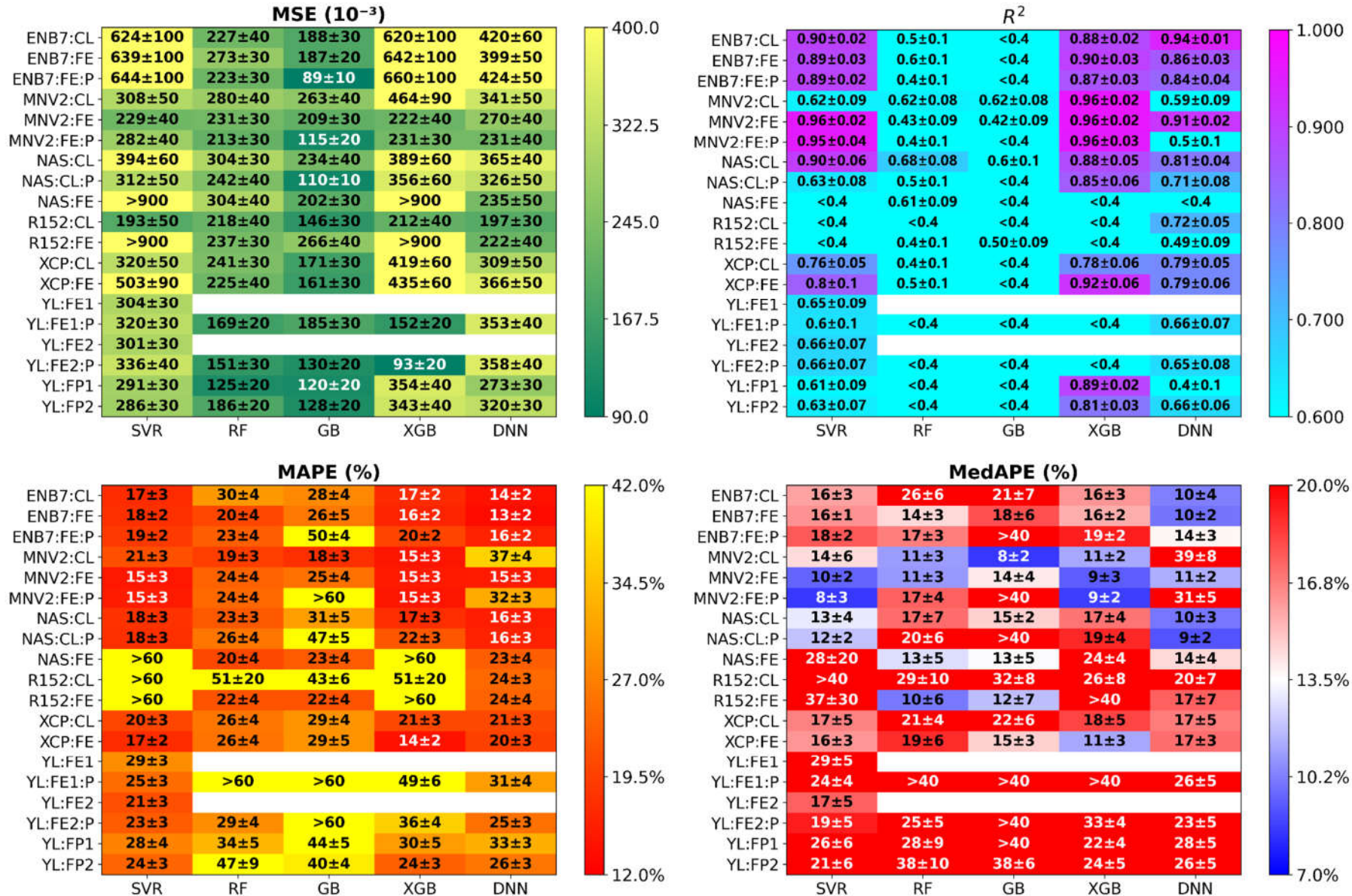
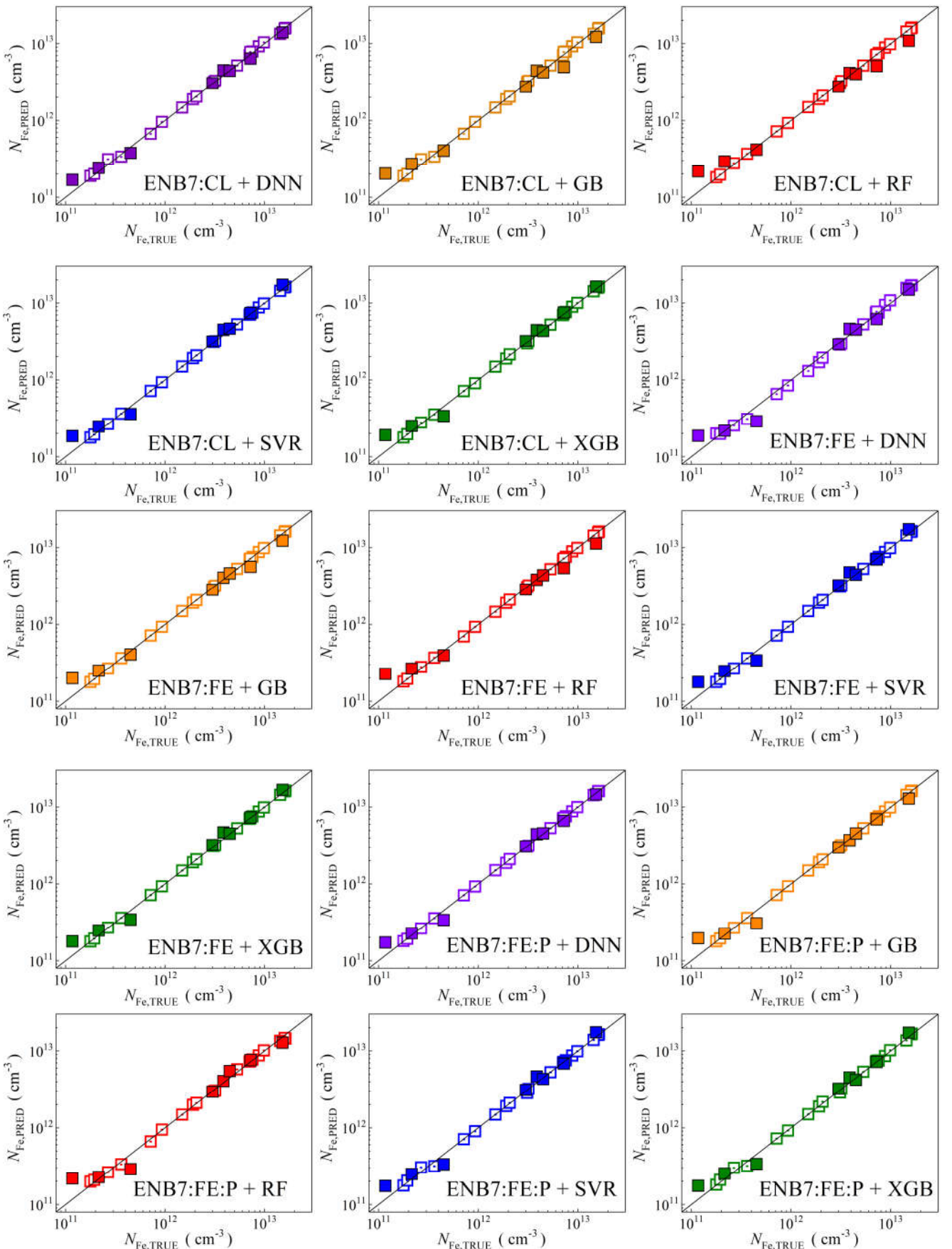
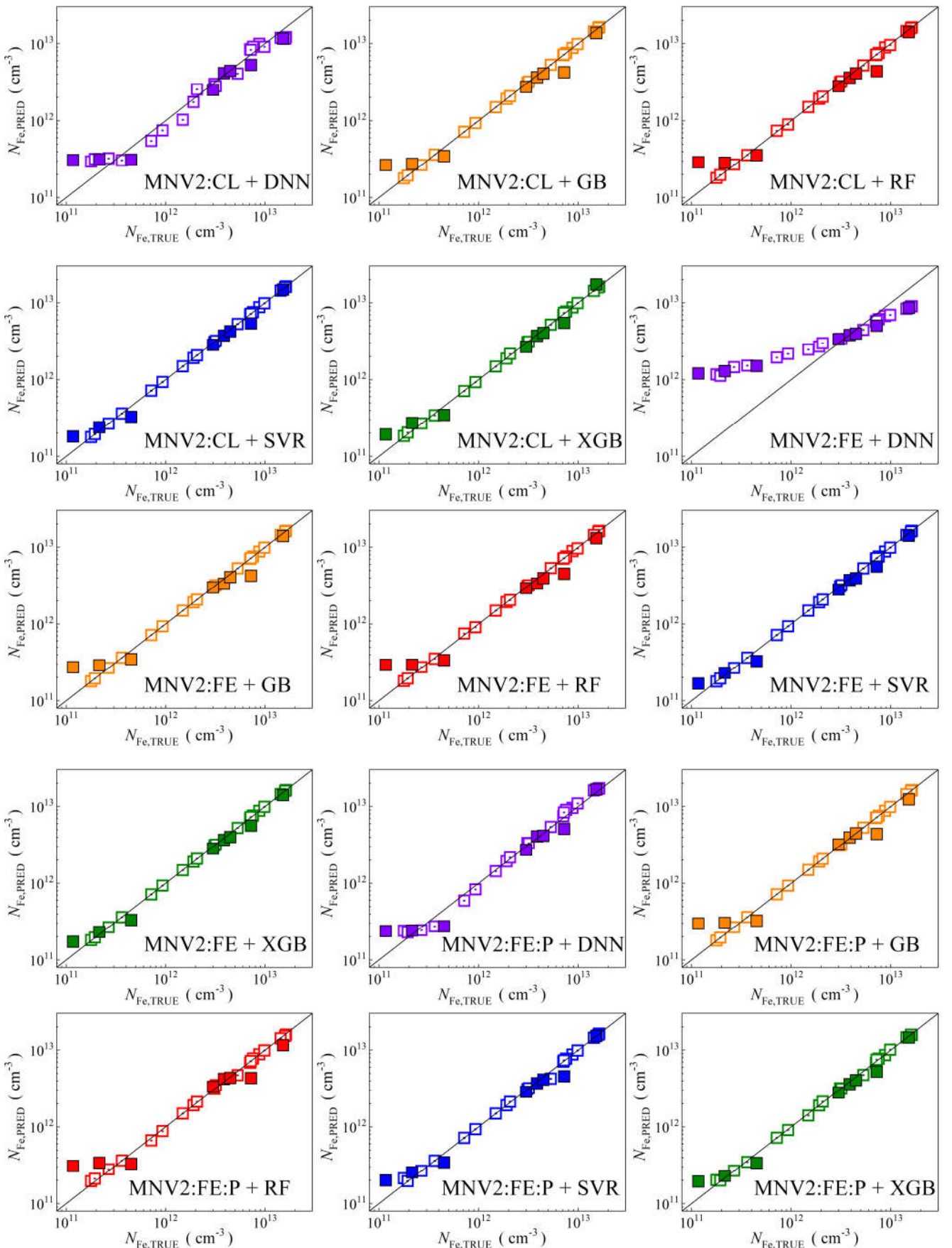
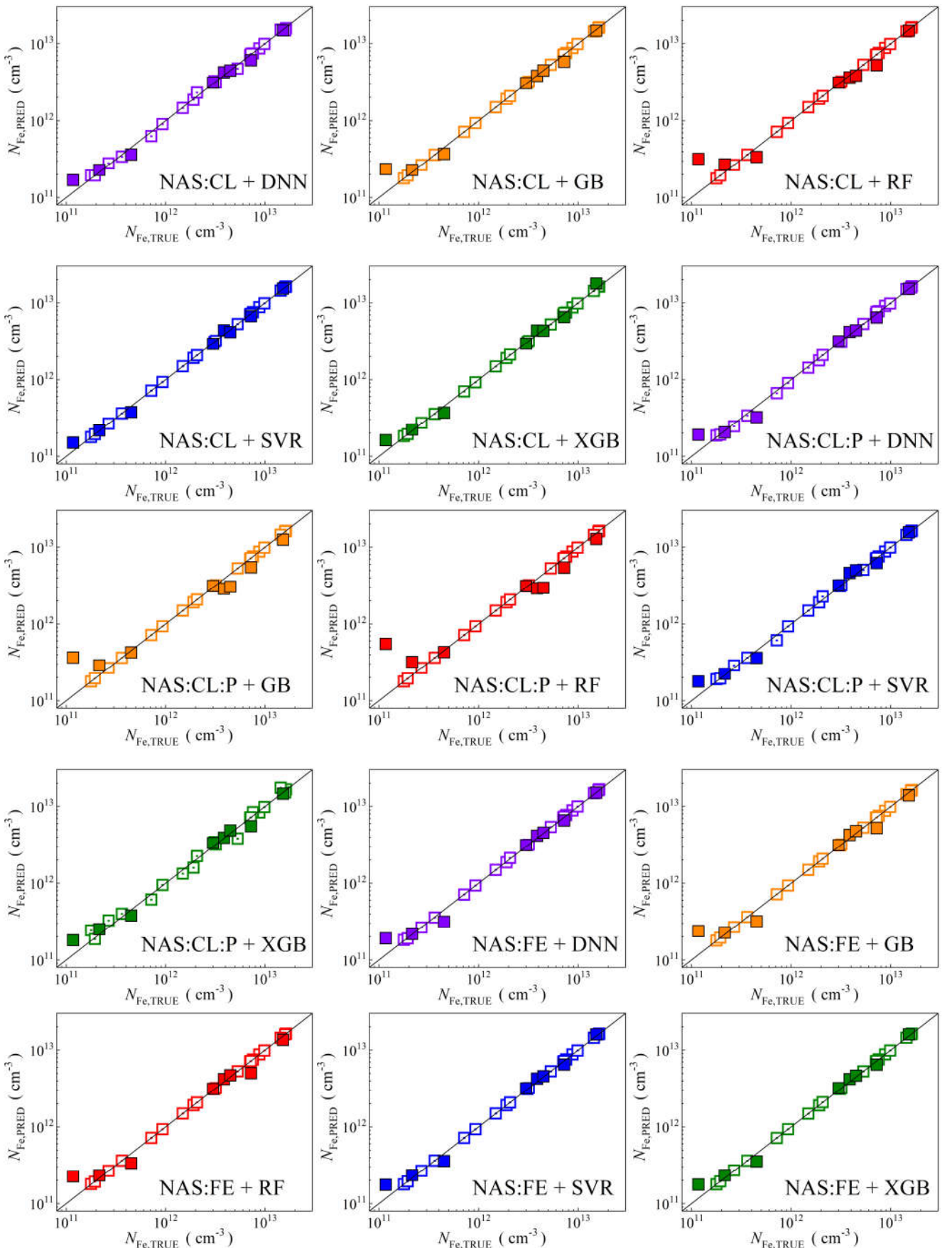
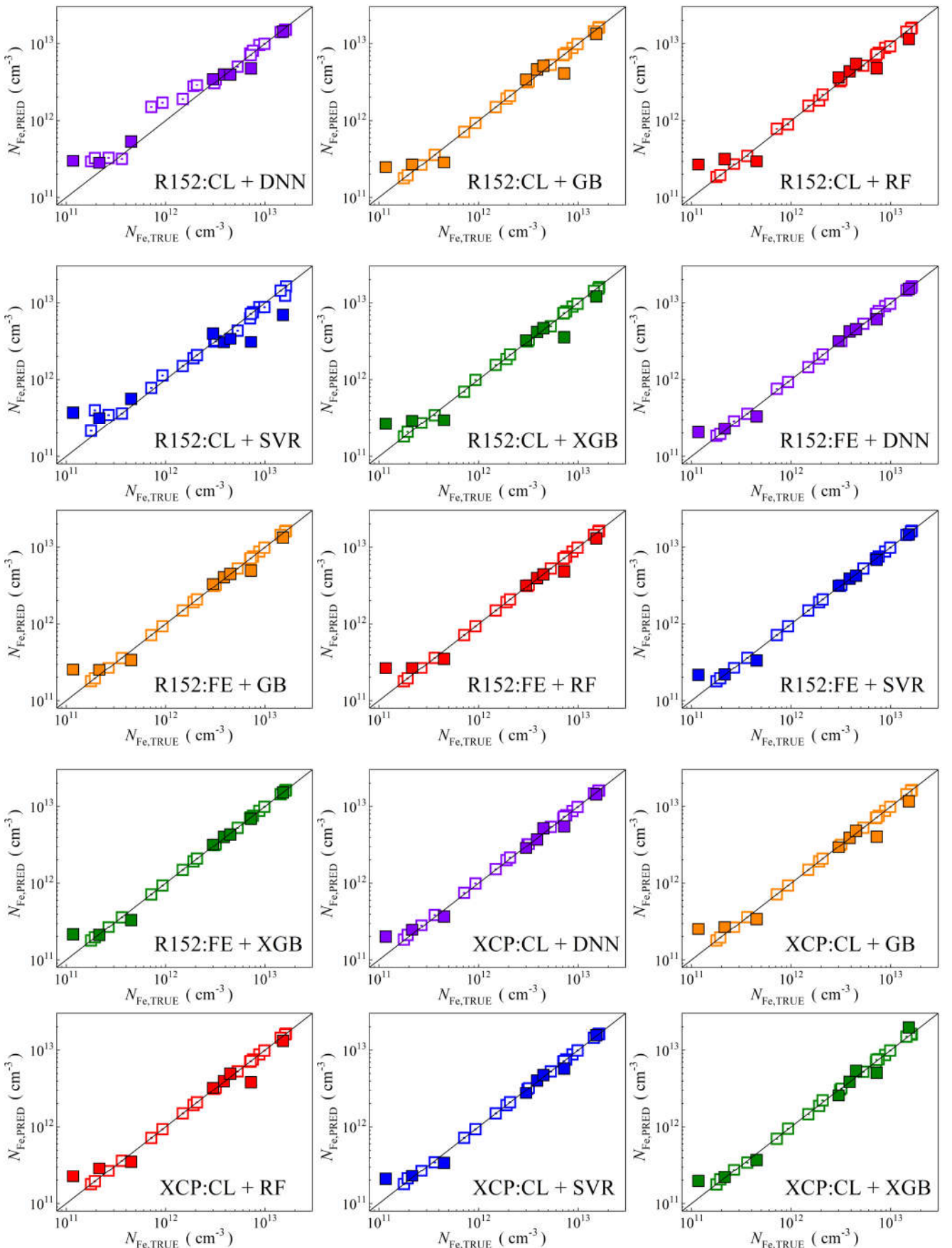


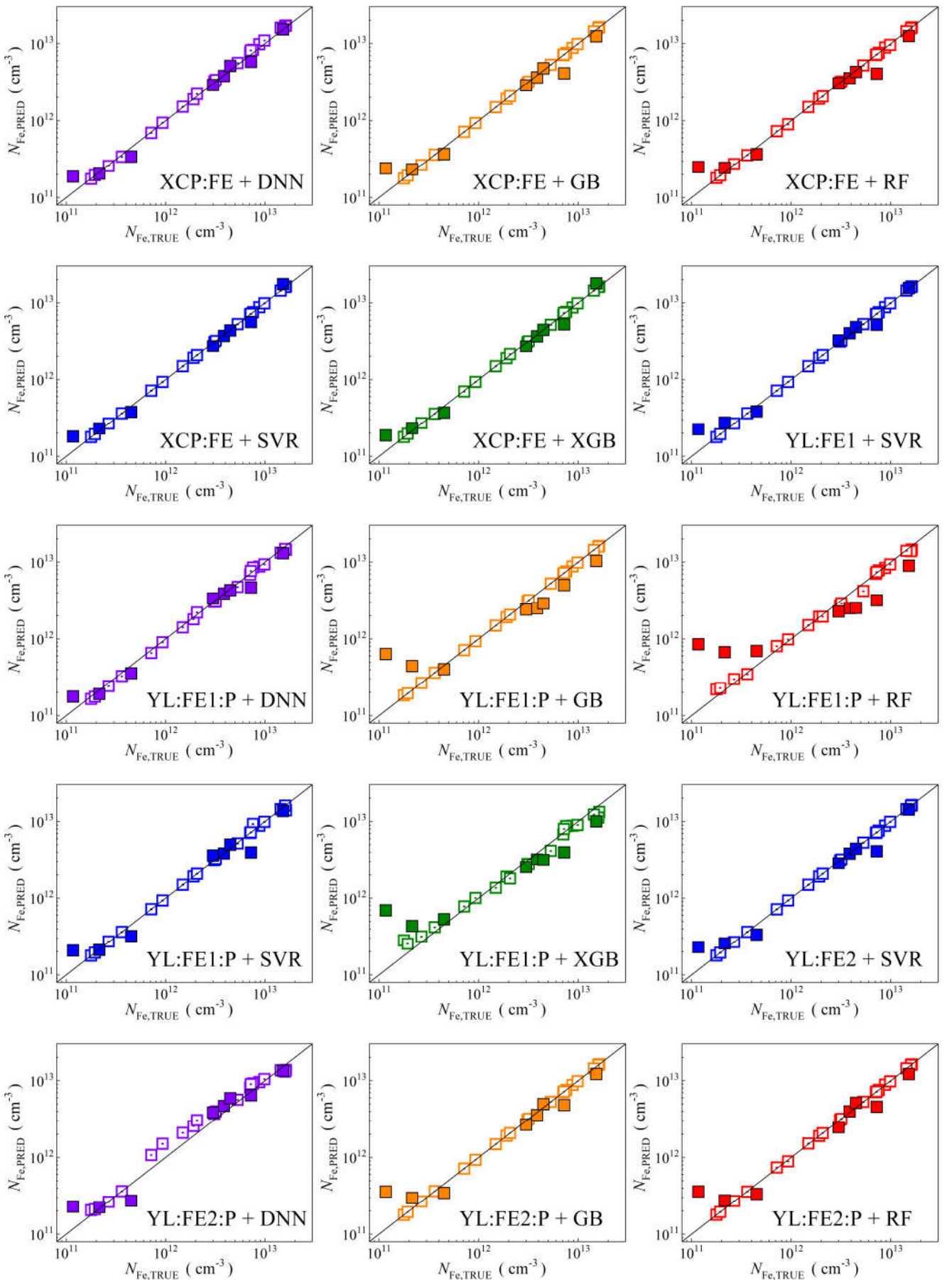
Fig. S7. Mean squared error, coefficient of determination, mean absolute percentage error, and median absolute percentage error for different combinations of computer vision models (vertical axis) and regression models (horizontal axis) during the **test phase with experimental dataset with post-hoc calibration**. The models were trained on a **simulated dataset**.











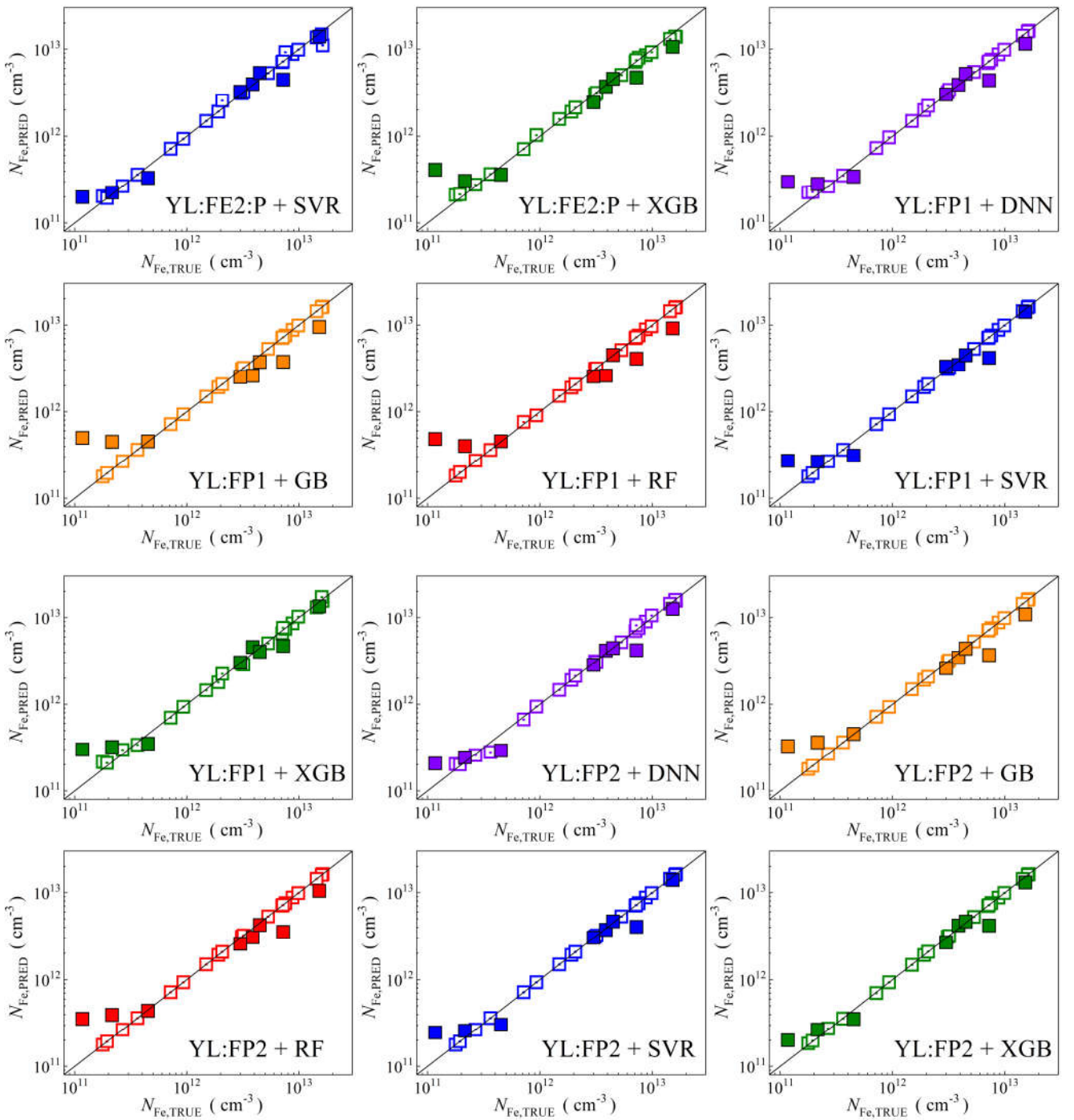


Fig. S8. Scatter plots compare the reference iron concentrations $N_{\text{Fe},\text{TRUE}}$ with ML-predicted values $N_{\text{Fe},\text{PRED}}$, obtained using feature vectors extracted from various computer vision models combined with different regression algorithms. The ML models were trained on a dataset derived from experimental measurements. The open and filled squares correspond to the training and test phases, respectively. The black lines are the identified lines serving as the references.

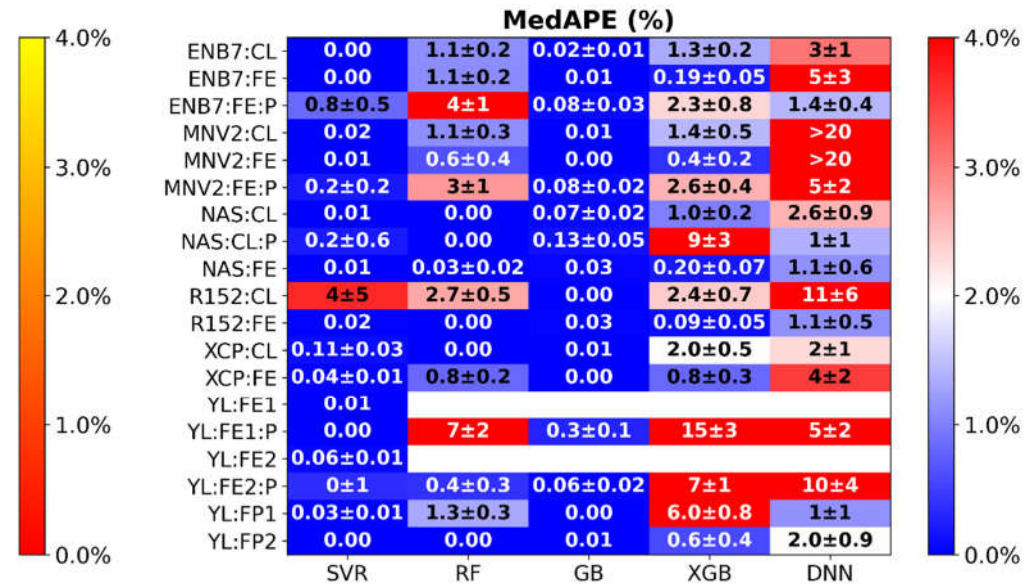
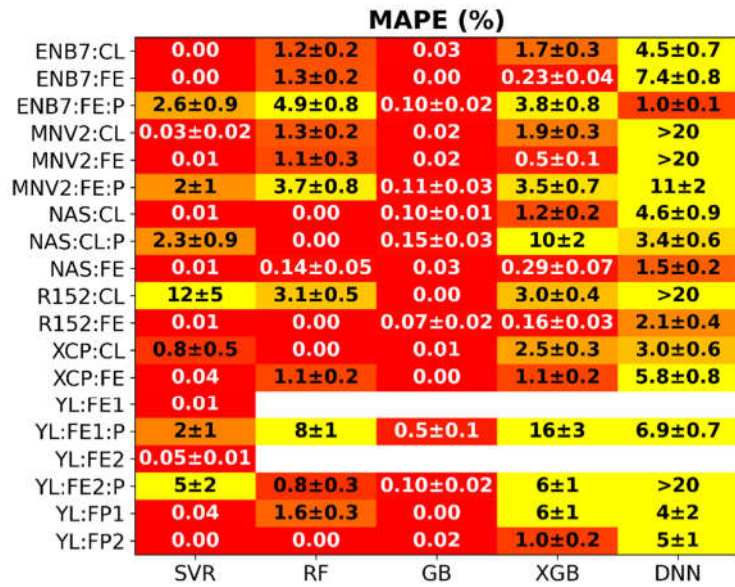
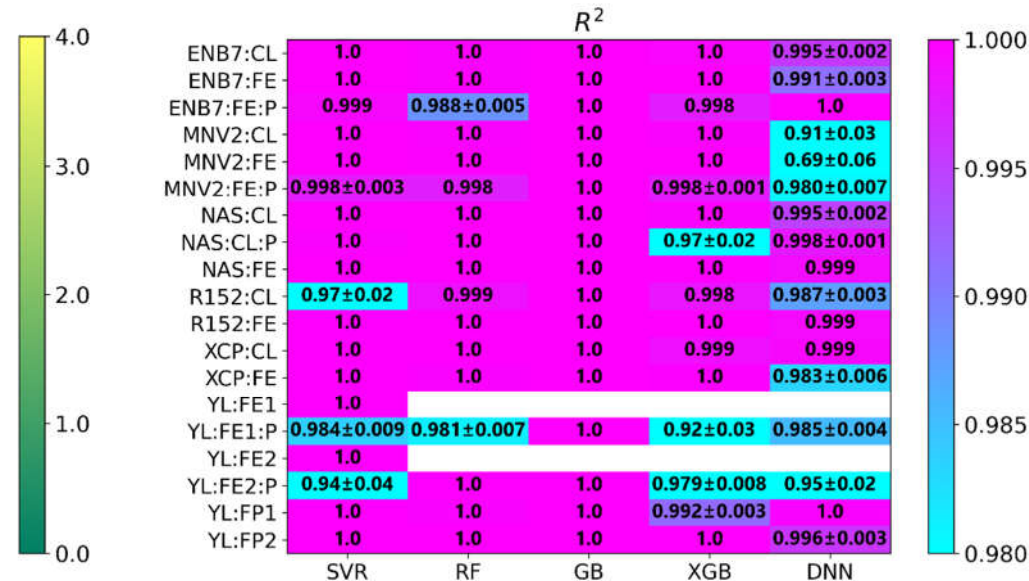
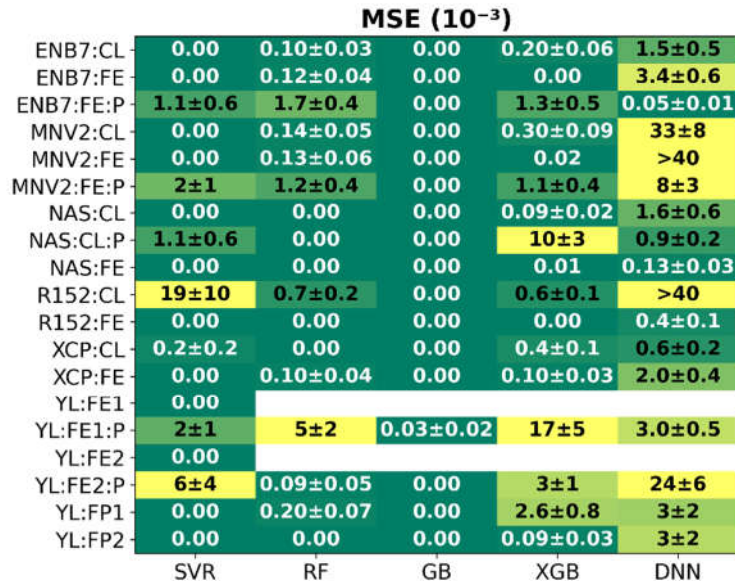


Fig. S9. Mean squared error, coefficient of determination, mean absolute percentage error, and median absolute percentage error for different combinations of computer vision models (vertical axis) and regression models (horizontal axis) during the **training phase**. The models were trained on an **experimental dataset**.

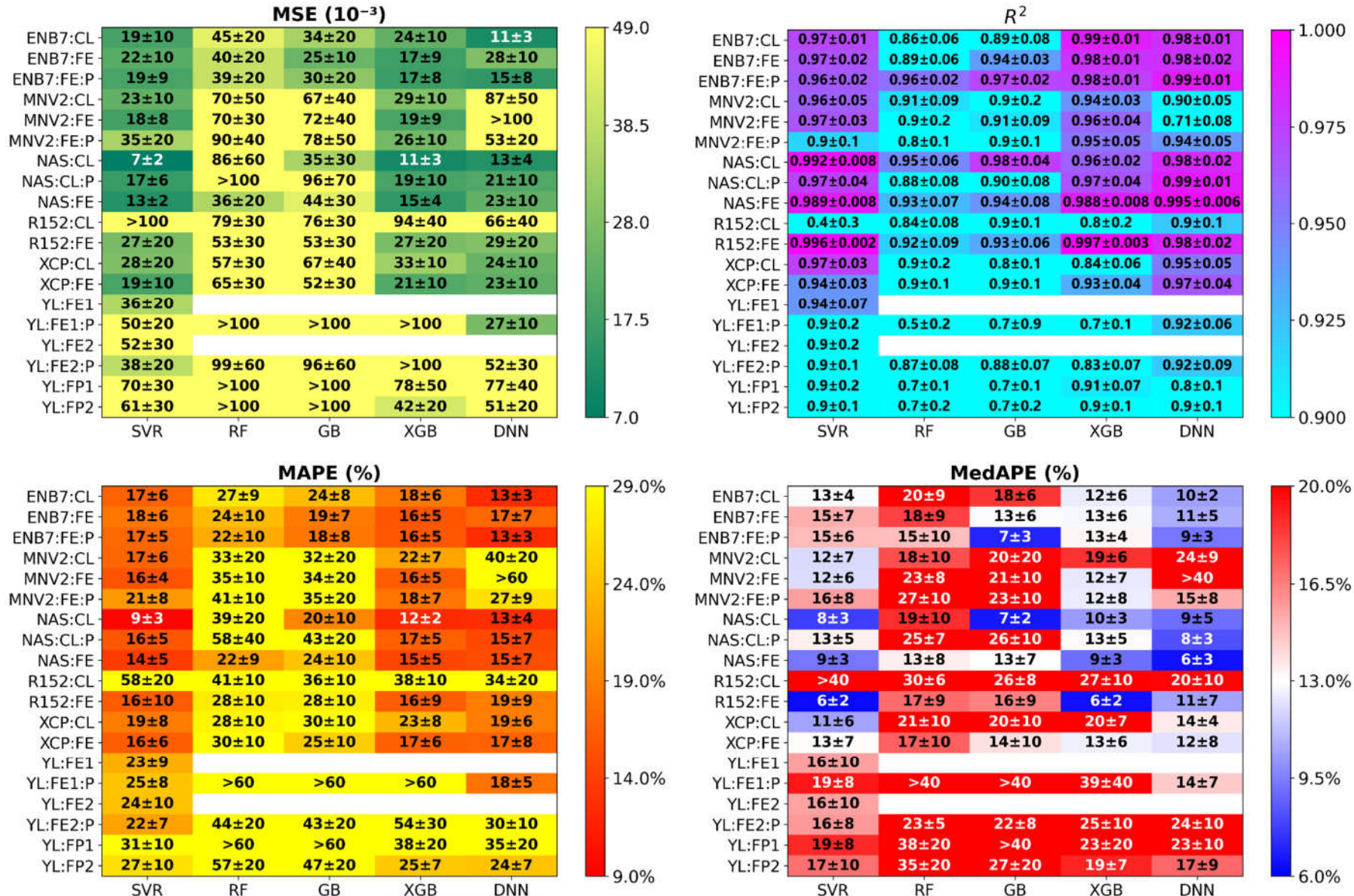


Fig. S10. Mean squared error, coefficient of determination, mean absolute percentage error, and median absolute percentage error for different combinations of computer vision models (vertical axis) and regression models (horizontal axis) during the test phase. The models were trained on an experimental dataset.